Utrecht University

Spin-wave cloaking

Master Thesis

Cas Korporaal

Theoretical physics

Supervisors:

Prof. Dr. R.A. Duine
Institute for Theoretical Physics

J.S. Harms
Institute for Theoretical Physics

Utrecht, July 9, 2023

Abstract

Spintronics is a fast growing new field in physics that has the potential to make a significant impact on all future electronics. It makes use of the electronic charge as well as its spin. Using this spin as a second degree of freedom will potentially increase performance and efficiency significantly. Possible information carriers can be introduced in the form of spin waves, which are periodic rotations of the spins along their original alignment. However, these spin waves can be distorted by impurities in spintronic devices. In this thesis we will use the field of transformation optics to cloak impurities from these spin waves. We will introduce anisotropies in the exchange interaction to accomplish this. By introducing a spintransfer torque in the system we will achieve almost perfect cloaking.

Contents

Chapter 1

Introduction

Every day electronics makes use of the charge of the electron, in so called electronic currents. These currents produce a lot of excess heat relative to the energy needed to maintain the current, therefore greatly increasing the energy cost of electronic devices and impeding the overall processing power of the device. The study of spintronics (spin electronics) tries to solve these issues by not relying on the charge of the electron but the spin, the intrinsic form of angular momentum carried by elementary particles. In an ordered magnetic material the atoms are arranged in a lattice all carrying a spin, making it possible for spin waves to occur. These spin waves are a periodic rotation of the spins along their original alignment, as shown in Figure 1.1. These waves can carry information and therefore lie at the basis of spintronics, opening up the possibility for wave-based computing (Chumak et al., 2015). This is a form of computing which allows operations with vectors instead of scalars, possibly opening the way to non-Boolean computing algorithms.

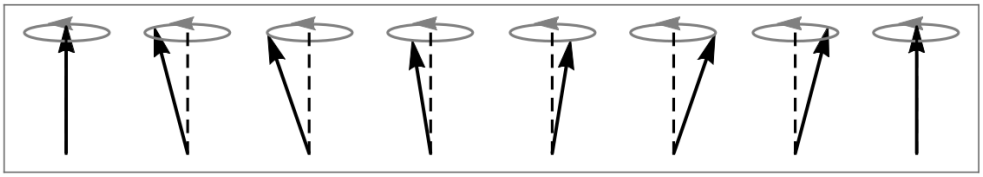

Figure 1.1: Graphical depiction of a spin wave in a ferromagnet. Here the spins are aligned along one axis. The rotation of the spins along this axis is called a spinwave. Taken from Heisteeg, 2016.

A problem with these waves is that they can be distorted by objects (impurities) or interfere after colliding with the edge of the magnetic medium. A possible solution for these distortions is to adapt the analytical techniques from transformation optics to try to steer these spin waves in the direction we want. Transformation optics is the theory of creating meta-materials, materials with properties not found in naturally occurring materials with properties that are spatially dependent, such that waves in this material behave as wanted. This theory was first developed in 2006 for electromagnetic waves and draws knowledge from general relativity (Leonhardt and Thomas G Philbin, 2006). In general relativity light can be bend due to the curvature of spacetime. Now using the underlying mathematics we can choose the spatially dependent properties of the meta-material such that the electromagnetic waves feel this curvature in the flat material.

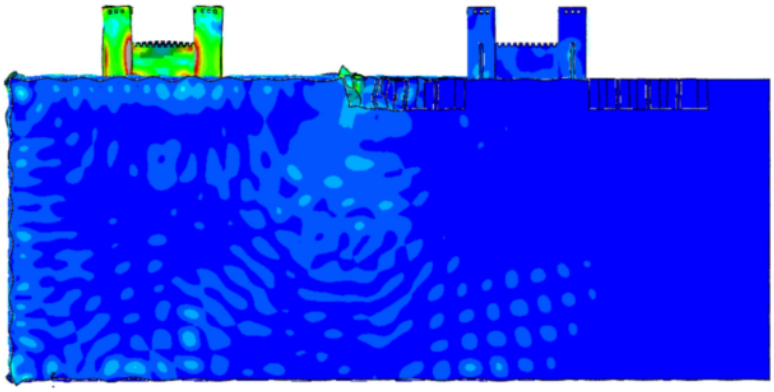

Figure 1.2: A normalised Von Mises stress field map. Here, the blue colour visualises minimal stress while red maximum stress. An earthquake is simulated in the middle. The building on the right protected by the rods experiences much less stress than the building on the left. Taken from Miniaci et al., 2016.

Since 2006 transformation optics has been used for novel ideas, one being a wave guide for earthquakes (Miniaci et al., 2016). Here rods are places in the ground in such a way that the seismic waves are diverted around a building or a city, thus negating the destructive forces in the area. This is clearly visualized in Figure 1.2. Here, a earthquake is simulated, originating from the middle. On the surface are two buildings. The one on the right is protected by the rods, while the left is not. It is clearly seen that the one on the left experiences a lot more stress (red and green colour) than the one on the right (blue colour).

Furthermore, experimentally a link has been made between the geometrical shape of a magnet and the emergence of a Dzyaloshinskii–Moriya interaction (DMI) (Sheka, 2021), an interaction which can influence spinwave propagation. Further strengthening the believe in the relation between geometry and spinwave propagation.

All this gives confidence to try using the ideas of transformation optics in magnetic materials, such that we can manipulate spin waves. In Elyasi et al., 2016 they tried to do this by changing the saturation magnetization or the gyromagnetic factor. Our goal in this thesis is the same. Instead of changing the saturation magnetization or gyromagnetic factor, we will change the exchange constant and introduce a spin transfer torque. In the thesis we will use cloaking (i.e. shielding regions in magnetic materials from the penetration of spin waves, such that the outgoing waves are the same as the incoming waves) as a good reference to test the theory in numerical simulations. We do this as it is more demanding that just diverting the spin waves, plus it is a nice tool to immediately see if the theory works by comparing the outgoing with the incoming waves.

This thesis is organized as follows. In Chapter 2 we review the theory behind transformation optics in detail. Here we will relate curvature to general coordinate transformations, which in return will give us the spatial dependence of the meta-material. Furthermore we will discuss the electromagnetic example because it shows the similarity between transformation optics and general relativity. This is because electromagnetic waves travel in vacuum as well in a dielectric medium, thus mimicking the curvature of space-time by making the medium spatially dependent. In Chapter 3 we will try to cloak spin waves in a ferromagnet. Here we start first with the

simplest description of spin waves i.e. only exchange, an anisotropy and a magnetic field. This description we will linearize along a spatial direction, such that we can easily apply transfromation optics. Then we will discuss the problems that occur with respect to the electromagnetic example. We will solve these problems by introducing a spin transfer torque in the system. After finding the spatial dependencies of the exchange constant and the spintransfertorque (Equations 3.18), we illustrate the results via the group velocity. Lastly we will show the numerical results (Figure 3.4). In Chapter 4 we will discuss an outlook of the antiferromagnetic case. We end in Chapter 5 with a conclusion and discussion of our results.

Chapter 2

Transformation optics

As discussed in the introduction there is a connection between geometrical shape or curvature of space time and how light waves behave. Transformation optics uses this connection to try to construct dielectric media such that it appears to light as if it was propagating in curved space-time. It is therefore of importance to understand the theory of general relativity and the underlying mathematics called differential geometry.

One of the core concepts in general relativity is that light travels along so called geodesics (a generalized notion of a straight line). An example is shown in Figure 2.1. Here on the left the normal situation (Cartesian) is shown, where light in a vacuum travels in straight lines along the green geodesics. On the right, the cloaking situation is shown. Here, all the geodesics are curved around a single hole in the middle of the grid, such that light never comes in contact with the spatial area in the middle, cloaking a potential object placed there.

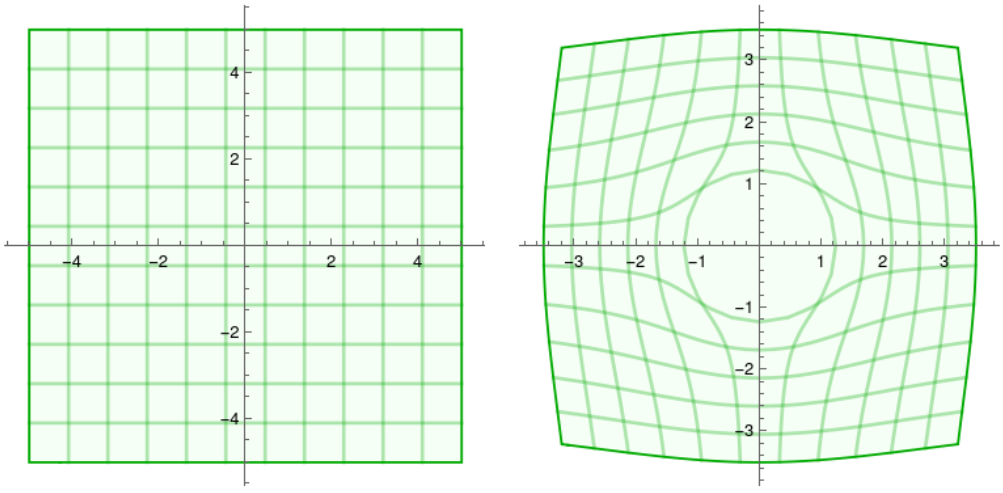

Figure 2.1: The left figure is in normal Cartesian coordinates in 2 dimensions, here the geodesics are the straight green lines. The figure on the right is in transformed coordinates such that an object in the middle is cloaked, since light still follows the green curves geodesics which don't intersect with the object in the middle.

All this is still allowed, since we can curve space-time. Transformation optics will try to manipulate light waves the other way around. Not by curving spacetime, but by absorbing this curvature into properties of the medium that govern the wave equation of light, such that for the light waves it is indistinguishable whether the medium is spatially uniform and in curved space-time or in flat space but spatially nonuniform. If this is the case, light will behave the same in both cases. Hence, we have found our wanted spatially dependent properties of the dielectric medium such that light is bend around the object in the middle.

Now, the question is how do we manifest this curvature in the plane? Again we can draw on the knowledge of general relativity. From general relativity we know that we can achieve this curvature through coordinate transformations, changing our flat (Minkowski) metric η to a curved metric g. This metric is of importance in differential geometry, in an object called the connection.

In the first paragraph we will discuss this connection and how this connection is used in the construction of a covariant derivative, something which is vital to express wave equations governing light, seismic or spin waves for instance. In the second paragraph we will discuss the electromagnetic example, since it explains the concept of transformation optics well. Also, it shows the ambiguity between curved spacetime in a vacuum and spatially non uniformity of a dielectric medium, since light can travel through a vacuum. Furthermore the problems that arise in the spin wave case are immediately clear by comparing it to the electromagnetic case.

2.1 Differential geometry

As discussed, curvature depends somehow on the metric g, which defines the geometry of the space. The problem is that it is not immediately clear if a space is curved from the metric. We will see that an object called the connection, which depends on the metric, will describe the curvature of the space. The Christoffel connection is given by:

$$\Gamma^{\nu}{}_{\mu\sigma} = \frac{1}{2} g^{\lambda\sigma}(\partial_\mu g_{\nu\sigma} + \partial_\nu g_{\sigma\mu} - \partial_\sigma g_{\mu\nu}). \tag{2.1}$$

It gives a way of relating vectors of nearby points. Now, a way of "seeing" this curvature is the concept of parallel transport. Simply said, this means keeping a vector constant along a path. This concept is shown in Figure 2.2. Here, in Figure 2.2a a vector is parallel transported from point A to B in flat space. Independent of the path taken, the vector at point B will point in the same direction as it started at point A. Now, in Figure 2.2b this is not the case anymore. Here, starting from the bottom left and parallel transporting the vector to the right then up will give a different result than starting from the bottom right transporting the vector to the left then up. So different paths will give different results. This is a clear indicator of a curved space, which a two-sphere clearly is.

A mathematical way of describing the rate of change of a vector in curved space, is with the covariant derivative. The covariant derivative is the generalization of the partial derivative in curved space and is given by:

$$\nabla_\mu V^\nu = \frac{\partial V^\nu}{\partial x^\mu} + \Gamma^\nu_{\mu\sigma} V^\sigma, \tag{2.2}$$

with V^ν a vector and $\Gamma^\nu_{\mu\sigma}$ the Cristoffel connection. The covariant derivative of a one-form is given by:

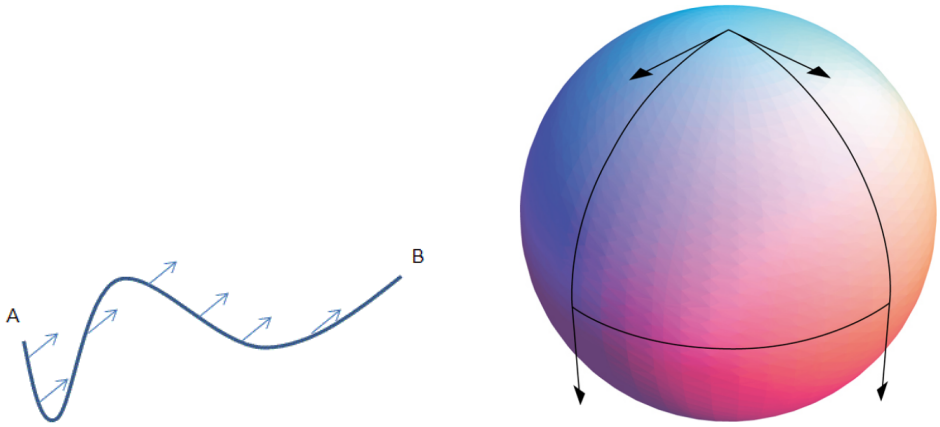

(a) (b)

Figure 2.2: (a) parallel transport in flat space versus (Source *Parallel Transport and Geodesic* n.d.) (b) parallel transport in curved space (Source Leonhardt and Thomas G. Philbin, 2008). In flat space the vector remains pointing in the same direction, whatever the path taken. In curved space the vector will chance direction depending on the path taken.

$$\nabla_\mu \omega_\nu = \frac{\partial \omega_\nu}{\partial x^\mu} - \Gamma^\lambda_{\mu\nu}\omega_\lambda, \tag{2.3}$$

with ω_ν a one form. Now given a curve $x^\mu(\lambda)$ the requirement of parallel transport is that the vector doesn't change along this curve, hence:

$$\frac{d}{d\lambda}V^\nu = \frac{dx^\mu}{d\lambda}\frac{\partial}{\partial x^\mu}V^\nu = 0. \tag{2.4}$$

Generalized to curved space this is equal to:

$$\frac{dx^\mu}{d\lambda}\nabla_\mu V^\nu = \frac{d}{d\lambda}V^\nu + \Gamma^\nu_{\sigma\rho}\frac{dx^\sigma}{d\lambda}V^\rho = 0. \tag{2.5}$$

This equation is known as the equation of parallel transport. Now, the notion of geodesics (generalized version of a straight line in curved space) can be explained rather well using parallel transport. It is defined as follows: A straight line is a path that parallel-transports its own tangent vector. Given that the tangent vector of a path $x^\mu(\lambda)$ is $dx^\mu/d\lambda$ and using Equation 2.5 we write the geodesic equation as:

$$\frac{d^2x^\mu}{d\lambda^2} + \Gamma^\mu_{\sigma\rho}\frac{dx^\sigma}{d\lambda}\frac{dx^\rho}{d\lambda} = 0. \tag{2.6}$$

For the rest of the thesis it is of importance to describe the covariant derivative in terms of the metric. To understand plane waves we need to know how the divergence transforms in curved space. In curved space the divergence is given by:

$$\nabla \cdot V = \frac{\partial V^\mu}{\partial x^\mu} + \Gamma^\mu_{\mu\lambda}V^\lambda, \tag{2.7}$$

where the Christoffel symbol can straightforwardly be written as:

$$\Gamma^{\mu}_{\mu\lambda} = \frac{1}{2}g^{\mu\sigma}(\partial_\mu g_{\lambda\sigma} + \partial_\lambda g_{\sigma\mu} - \partial_\sigma g_{\mu\lambda}) = \frac{1}{2}g^{\mu\sigma}\partial_\lambda g_{\sigma\mu} = \frac{1}{\sqrt{g}}\partial_\lambda\sqrt{g}. \tag{2.8}$$

Here we used the symmetry of the metric tensor to cancel the first and last terms in the brackets to get to the second equality. The third equality follows from the variational derivative of the determinant of the metric $\frac{1}{\sqrt{g}}\delta\sqrt{g} = \frac{1}{2}g^{\mu\sigma}\delta g_{\sigma\mu}$. Hence the divergence can be written as:

$$\nabla \cdot V = \frac{1}{\sqrt{g}}\partial_\mu(\sqrt{g}V^\mu). \tag{2.9}$$

Another important term that we have to describe is the d'Alembert operator on a scalar. Using the just obtained equation of the divergence and Equation 2.3, we can do as follows. The D'Alambert operator is written as:

$$\Box\phi = g^{\mu\nu}\nabla_\nu\nabla_\mu = \Big[g^{\mu\alpha}\partial_\mu - g^{\mu\nu}\Gamma^{\alpha}_{\mu\nu}\Big]\partial_\alpha\phi. \tag{2.10}$$

Here, the second term can be written as:

$$\begin{aligned} -g^{\mu\nu}\Gamma^{\alpha}_{\mu\nu} &= -g^{\mu\nu}\frac{1}{2}g^{\alpha\sigma}\Big(\partial_\mu g_{\nu\sigma} + \partial_\nu g_{\sigma\mu} - \partial_\sigma g_{\mu\nu}\Big) \\ &= -g^{\alpha\sigma}g^{\mu\nu}\partial_\mu g_{\nu\sigma} + \frac{1}{2}g^{\alpha\sigma}g^{\mu\nu}\partial_\sigma g_{\mu\nu}. \end{aligned} \tag{2.11}$$

From Equation 2.8 we immediately see that the second term is written as $g^{\alpha\sigma}\frac{1}{\sqrt{g}}\partial_\sigma\sqrt{g}$. Using Leibniz rule, the first term in Equation 2.11 can be written as $g^{\mu\nu}g_{\nu\sigma}\partial_\mu g^{\alpha\sigma} = \delta^\mu_\nu\partial_\mu g^{\alpha\sigma} = \partial_\mu g^{\alpha\mu}$, using that the total derivative $\partial_\mu(g_{\nu\sigma}g^{\alpha\sigma}) = \partial_\mu(\delta^\alpha_\nu)$ equals zero. Combining all these terms will result in our final equation for the D'Alambert operator:

$$\Box\phi = \Big[g^{\sigma\alpha}\partial_\sigma + (\partial_\sigma g^{\sigma\alpha}) + g^{\alpha\sigma}\frac{1}{\sqrt{g}}\partial_\sigma\sqrt{g}\Big]\partial_\alpha\phi = \frac{1}{\sqrt{g}}\partial_\sigma(\sqrt{g}g^{\sigma\alpha}\partial_\alpha\phi). \tag{2.12}$$

2.2 Cloaking in electromagnetism

To see the connection between transformation optics and curvature, it is best to study the electromagnetic example first. This is because electromagnetic waves can propagate through vacuum as well as a dielectric medium. Here one can imagine that the macroscopic vacuum is curved while the dielectric medium is small enough to be locally flat. Electromagnetic waves can be described by Maxwell's equations, which describe how the electric field strength E and the magnetic induction B behave:

$$\begin{aligned} \nabla \cdot E &= \frac{\rho}{\epsilon_0}, & \nabla \cdot\ B &= 0, \\ \nabla \times E &= -\frac{\partial B}{\partial t}, & \nabla \times B &= \frac{\partial E}{\partial t} + \mu_0 j, \end{aligned} \tag{2.13}$$

with ϵ_0 the electric permittivity, μ_0 the magnetic permeability. The speed of light in a vacuum is set to 1. Furthermore, the charge and current densities are ρ and j, respectively. In the previous section we have seen how these divergences are expressed in curved space. Using that the curls are expressed simply as $(\nabla \times V)^i = \epsilon^{ijk}\partial_j V_k$, with V a vector and ϵ^{ijk} the Levi Civita tensor, we can write Maxwell's equations as:

$$\frac{1}{\sqrt{g}}\partial_i(\sqrt{g}E^i) = \frac{\rho}{\epsilon_0}, \qquad \frac{1}{\sqrt{g}}\partial_i(\sqrt{g}B^i) = 0,$$
$$\epsilon^{ijk}\partial_j E_k = -\frac{\partial B^i}{\partial t}, \qquad \epsilon^{ijk}\partial_j B_k = \frac{\partial E^i}{\partial t} + \mu_0 j^i. \tag{2.14}$$

With the tools developed from differential geometry, one can see that it is straightforward to express these equations in curved space. To arrive at our desired final equations we will lower all the indices for the electric field strength E and magnetic induction B, using the equality $\epsilon^{ijk} = \pm\frac{1}{\sqrt{g}}[ijk]$, with $[ijk]$ the parity. All this will yield the following equations:

$$\frac{1}{\sqrt{g}}\partial_i(\sqrt{g}g^{ij}E_j) = \frac{\rho}{\epsilon_0}, \qquad \frac{1}{\sqrt{g}}\partial_i(\sqrt{g}g^{ij}B_j) = 0,$$
$$[ijk]\partial_j E_k = -\frac{\partial \pm \sqrt{g}g^{ij}B_j}{\partial t}, \qquad [ijk]\partial_j B_k = \frac{\partial \pm \sqrt{g}g^{ij}E_j}{\partial t} + \mu_0\sqrt{g}j^i. \tag{2.15}$$

On the other hand, Maxwell's equations in a dielectric medium in Cartesian (flat) coordinates are governed by:

$$\partial_i D^i = \rho, \qquad \partial_i(B^i) = 0,$$
$$[ijk]\partial_j E_k = -\frac{\partial B^i}{\partial t}, \qquad [ijk]\partial_j H_k = \frac{\partial D^i}{\partial t} + j^i. \tag{2.16}$$

Here, D is the displacement field and H is the magnetization field. For materials without polarization and magnetization the relations between E, B and D, H are respectively:

$$D = \epsilon_0 E, \qquad H = \frac{1}{\mu_0}B \tag{2.17}$$

Now to express Maxwell's equations in a dielectric medium as if the waves were propagating in a curved vacuum, we can rescale the charge and current densities with $\sqrt{g}$ and choose our displacement and magnetization field such that Equation 2.16 is equal to Equation 2.15. This is accomplished by choosing D and H as:

$$D^i = \epsilon_0\epsilon^{ij}E_i, \qquad B^i = \mu_0\mu^{ij}H_j, \qquad \epsilon^{ij} = \mu^{ij} = \pm\sqrt{g}g^{ij}. \tag{2.18}$$

Equation 2.18 is the final result. Here we can see that by introducing anisotropies in ϵ^{ij} and μ^{ij} the electromagnetic waves do not see the difference between geometries and the dielectric media. Here geometries can appear as dielectric media or dielectric media can appear as geometries. In this thesis we are interested in the latter. The idea is that, for instance, we will choose the geometry of Figure 2.1, derive the spatial dependencies of our D and H and simulate the wave propagation in these media.

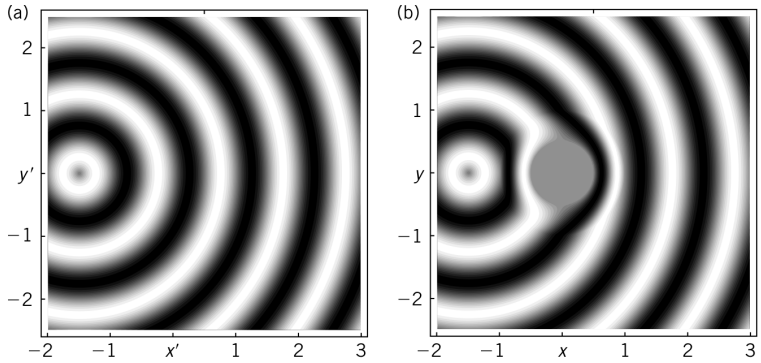

Figure 2.3: Electromagnetic wave propagation in (a) a spatially uniform dielectric medium and (b) a spatially dependent dielectric medium, such that the waves are bend around the object positioned at (x,y). Only in the region around this object in a radius of 1 behave different than in (a), thus the object is successfully cloaked.

An example of such simulations is been done in Leonhardt and Thomas G. Philbin, 2008. Here, they simulated electromagnetic wave propagation in a dielectric medium with such geometry as in Figure 2.1, the results are shown in Figure 2.3. Here, in the figure on the right the cloaking of an object is seen. The figure on the left serves as a reverence for wave propagation in a spatially uniform dielectric medium. The cloaking mechanism can be seen by comparing the two figures. Only in a small radius around the gray object are the waves propagated differently.

Numerical simulations are also conducted in Cummer et al., 2006 and recently cloaking is also achieved in an experimental setting (Schurig et al., 2006). The setup and results are seen in Figure 2.4. Here, a 2D microwave cloaking structure is used with varying material parameters. Results show that there is less interference from the conducting core when cloaking is used.

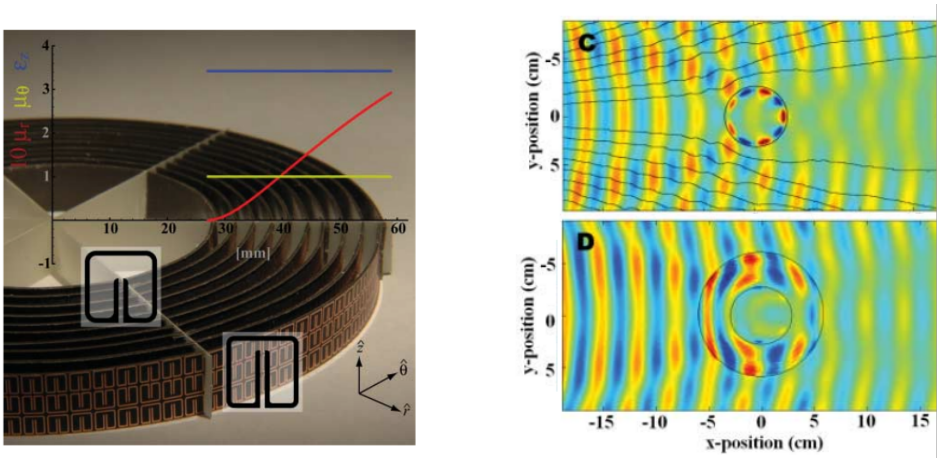

(a) **(b)**

Figure 2.4: (a) experimental setup. (b) results of electromagnetic wave propagation. The top result is without cloaking, the bottom result is with cloaking.

Chapter 3

Spin wave cloaking in ferromagnets

In this chapter we will discuss spin waves in ferromagnets. Ferromagnets are a special kind of magnet, in the sense that in the ground state all magnetic moments will point in the same direction, thus making them an ideal candidate to facilitate spin waves. Whether a material is ferromagnetic or anti-ferromagnetic is determined via the exchange interaction. Is the exchange interaction J strictly positive the material is ferromagnetic, otherwise it is anti-ferromagnetic. This is best seen from the Hamiltonian given by:

$$H = -\frac{J}{2}\sum_i \sum_\delta \vec{S}_i \cdot \vec{S}_{i+\delta}. \tag{3.1}$$

Here, $\vec{S}_i$ is the spin on position i, which interacts with its nearest neighbours on positions $i+\delta$. Clearly, when the exchange interaction $J > 0$ the energy is minimized when all spins are aligned in the same direction. The equations of motion, via Erhenfest's theorem, are given as:

$$\frac{\partial \vec{S}_i}{\partial t} = -\vec{S}_i \times \frac{\partial H}{\partial \vec{S}_i}. \tag{3.2}$$

In the semi-classical approximation the spins $\vec{S}$ on a lattice are replaced by a magnetization vector field $\vec{M}$ which is continuous in space and orientation. This approximation is valid when the characteristic length scale on which the magnetization changes its direction is large compared to the distance of the spins (Krueger, 2012). In this limit Equation 3.2 will transform to:

$$\frac{d\vec{M}}{dt} = -\gamma \vec{M} \times \vec{H}_{eff}, \tag{3.3}$$

with γ the gyromagnetic ratio and the effective field $\vec{H}_{eff}$ in the continuum limit given by:

$$\vec{H}_{eff} = -\frac{1}{\mu_0}\frac{\delta E}{\delta \vec{M}}. \tag{3.4}$$

Equation 3.3 describes how our spin waves will propagate, where E contains the exchange interaction and other magnetic interactions. These interactions will be discussed in detail in the next section. Also, in the this section we will linearize this equation for the most simplest case of energy E, such that we get an equation for spin waves similar to the electromagnetic example.

This equation is transformed with the tools from transformation optics. If we try to connect the curved equations with the Cartesian ones, we will see that problems arise. We will solve these problems by introducing a spin transfer torque. To simulate the spin waves in Mathematica effectively we will make our equations of motion dimensionless. Furthermore, we will illustrate the theory via the group velocity to see that the spin waves are indeed curved around the introduced object. Lastly we will explain our boundary conditions used in Mathematica and show our results.

3.1 Linearized equations of motion

To arrive at the simplest equations of motion (EOM), we will use Equation 3.3 with energy E:

$$E = \int d\vec{\rho}\Big\{\vec{M}(\vec{\rho})J\nabla^2\vec{M}(\vec{\rho}) - \frac{K_z M_z^2}{2} - B_z M_z\Big\}, \tag{3.5}$$

with $K_z M_z^2/2$ the uniaxial anisotropy energy and $B_z M_z$ the magnetic field energy in the $\hat{z}$ direction. To linearize the EOM along the $\hat{z}$ direction we define the total magnetization as:

$$\vec{M} = \vec{M}_0 + \vec{M}_d = M_s\begin{pmatrix}0\\0\\1\end{pmatrix} + M_s\begin{pmatrix}\delta M_x\\ \delta M_y\\ 0\end{pmatrix}, \tag{3.6}$$

with $\vec{M}_0$, $\vec{M}_d$ respectively the static and the dynamic part of the magnetization. The saturation magnetization is indicated by M_s. To calculate the effective field, we use the definition of the functional derivative as stated in Krueger, 2012, which yields, after integrating over all of ρ, the following functional derivative:

$$\frac{\delta E[\vec{M}(\vec{\rho})]}{\delta\vec{M}(\vec{\rho}_0)} = -J\nabla^2\vec{M}(\rho_0)\cdot\hat{e}_x - J\nabla^2\vec{M}(\rho_0)\cdot\hat{e}_y - J\nabla^2\vec{M}(\rho_0)\cdot\hat{e}_z - K_z M_z\hat{e}_z - B_z\hat{e}_z. \tag{3.7}$$

Here, ρ and ρ_0 are the spatial coordinates and a specific point in space, respectively. Now, substituting Equation 3.7 in Equation 3.3 yields:

$$\begin{pmatrix}\delta\dot{M}_x\\ \delta\dot{M}_y\end{pmatrix} = \begin{pmatrix}2J\nabla^2\delta M_y - B_z\delta M_y - K_z M_s\delta M_y\\ -2J\nabla^2\delta M_x + B_z\delta M_x + K_z M_s\delta M_x\end{pmatrix}. \tag{3.8}$$

These equations describe the EOM of the spin waves perfectly, but would be difficult to transform to curved space. We will solve this by using the transformation:

$$T:\mathbb{R}^2\to\mathbb{C};\quad T\left(\begin{pmatrix}\delta M_x\\ \delta M_y\end{pmatrix}\right) = \begin{pmatrix}\delta M_x\\ -\delta M_y\end{pmatrix} = \phi(\rho,t). \tag{3.9}$$

Using this transformation, we write the EOM as:

$$i\frac{\partial}{\partial t}\phi = \frac{\gamma}{\mu_0}\Big\{-2J\nabla^2 + B_z + K_z M_s\Big\}\phi. \tag{3.10}$$

To solve this equation, we make the following ansatz: $\phi = \vec{A}e^{i(\vec{k}\cdot\vec{\rho}-\omega t)}$, where ω is the angular frequency and $\vec{k}$ the wavevector. With this ansatz we find the following dispersion relation:

$$\omega_k = \frac{\gamma}{\mu_0}\Big\{2Jk^2 + B_z + K_z M_s\Big\}. \tag{3.11}$$

We can see that Equation 3.10 is in the same form as Maxwell's equations discussed in the previous chapter. By grouping the magnetic field and the uniaxial anisotropy energy in one term (B), we write equation 3.10 in curved space as:

$$\begin{aligned} i\frac{\partial}{\partial t}\phi &= -J\frac{\gamma}{\mu_0}\frac{1}{\sqrt{g}}\partial_k[\sqrt{g}g^{kj}\partial_j\phi] + B\frac{\gamma}{\mu_0}\phi \\ &= -J\frac{\gamma}{\mu_0}\Big\{\frac{1}{\sqrt{g}}\partial_k[\sqrt{g}g^{kj}]\partial_j + g^{kj}\partial_k\partial_j\Big\}\phi + B\frac{\gamma}{\mu_0}\phi, \end{aligned} \tag{3.12}$$

and in Cartesian coordinates (flat space) as:

$$i\frac{\partial}{\partial t}\phi = -J\frac{\gamma}{\mu_0}\partial_j^2\phi + B\frac{\gamma}{\mu_0}\phi. \tag{3.13}$$

To have the spin waves in the Cartesian plane behave as if there were in the curved space, we need to absorb the extra terms into the exchange interaction J in Cartesian space, such that the two equations look the same. Here, we arrive at a problem. We see that this is not possible for all geometries because we have the extra term $\partial_k[\sqrt{g}g^{kj}]\partial_j$, which has not counterpart in the Cartesian plane. Only when this term is equal to zero it is possible to make both equations equivalent. To cope with this problem we will introduce a spin transfer torque, which will yield an extra divergence in the EOM such that we can deal with the extra term.

3.2 Introducing the spin transfer torque

The spin transfer torque is an effect in which the orientation of the spins in a magnetic material can be influenced using a spin polarized current. Normally an electronic current is unpolarized, meaning the distribution of spins of the electrons is not biased (consisting of spins 50% up and 50% down). When a polarized current is used, the angular momentum of the spins is transferred to the spins in the magnetic material thus influencing its magnetic moments. There are two kinds of spin transfer torques (STT's), an adiabatic one and a non-adiabetic one. These two kinds of STT's are explained fully in Krueger, 2012. Adding the two STT's to the equations of motion will yield:

$$\frac{d\vec{M}}{dt} = -\gamma\vec{M}\times H_{eff}\underbrace{-\frac{b_j}{M_s^2}\vec{M}\times(\vec{M}\times(\vec{j}\vec{\nabla})\vec{M})}_{\text{adiabatic spin torque}}\underbrace{-\frac{\xi b_j}{M_s}\vec{M}\times(\vec{j}\vec{\nabla})\vec{M}}_{\text{non-adiabatic spin torque}}, \tag{3.14}$$

where $\vec{j}$ the current density, $b_j = \mu_B P/[eM_s(1+\xi^2)]$ the coupling constant between the current and the magnetization, P the polarization of the current and ξ the damping parameter in the non-adiabatic STT. If we again linearize this equations via the same steps as explained in the previous section, we obtain the following equation of motion in Cartisian space:

$$i(\frac{\partial}{\partial t} + u^j\partial_j)\phi = \frac{\gamma}{\mu_0}\Big\{-J\partial_j^2 + B + \xi u^j\partial_j\Big\}\phi, \tag{3.15}$$

with the generalized current $\vec{u} = b_j\vec{j}$. Here we see that we obtained the needed divergences. To absorb the divergence in Equation 3.12 we only need the real one, the non-adiabatic one. To get rid of the imaginary adiabatic STT, we will decouple the two via the limit $\vec{u}\to 0$ and set the dampening parameter to $\xi = v^i/u^i$. Where $\vec{v}$ is now the non-adiabatic current. This results in our final equation of motion:

$$i\frac{\partial}{\partial t}\phi = \frac{\gamma}{\mu_0}\Big\{-J\partial_j^2 + B + v^j\partial_j\Big\}\phi. \tag{3.16}$$

In curved coordinates this is equal to:

$$i\frac{\partial}{\partial t}\phi = \frac{\gamma}{\mu_0}\Big\{-J\frac{1}{\sqrt{g}}\Big[\partial_k[\sqrt{g}g^{kj}]\partial_j + \sqrt{g}g^{kj}\partial_k\partial_j\Big] + B + v_k g^{kj}\partial_j\Big\}\phi. \tag{3.17}$$

To make these equations equivalent we need the following dependencies of the constants:

$$\begin{aligned} J^{kj} &= g^{kj}J, \\ B &= B, \\ v^j &= -\frac{J}{\sqrt{g}}\partial_k[\sqrt{g}g^{kj}] + v_k g^{kj}. \end{aligned} \tag{3.18}$$

This is our final result for spin waves in a ferromagnet. With these dependencies we can now choose any geometry accompanied by a metric g such that the spin waves will follow the geodesics of the geometry.

3.3 Numerical results

To reinforce our theoretical results, we will simulate our results in Mathematica. But before we can do that, we will make it ourselves somewhat easier by first making the results dimensionless. This will make programming more easy. After we have done this we will introduce the coordinate transformation which lies at the basis of the geometry seen in Figure 2.1. This will give us concrete formulas to work with in the simulations. Lastly the results are shown.

3.3.1 Dimensionless equation of motion

To make the equation of motion dimensionless, we will introduce transformations in time t and space $\vec{x}$. First we will introduce the transformation in the time as: $t \to \tilde{t} = u_0/(\gamma B)$. This will transform the partial time derivative as: $\partial_t = \frac{\partial\tilde{t}}{\partial t}\partial_{\tilde{t}} = u_0/(\gamma B)\partial_{\tilde{t}}$, transforming the EOM as:

$$i\frac{\partial}{\partial t}\phi = -\frac{J}{B}\partial_j^2 + 1 + \frac{v^j}{B}\partial_j\phi. \tag{3.19}$$

Secondly we will introduce the spatial transformation $x \to \tilde{x} = \sqrt{J/(B\Lambda)}$ with Λ a dimensionless exchange constant. This will result in:

$$i\frac{\partial}{\partial t}\phi = -\Lambda\partial_j^2 + 1 + v^j\sqrt{\frac{\Lambda}{BJ}}\partial_j\phi. \tag{3.20}$$

This is our dimensionless EOM with $\vec{\beta} = \vec{v}\sqrt{\frac{\Lambda}{BJ}}$ the dimensionless current.

3.3.2 Coordinate transformation

Previous we have worked with a general geometry with metric g_{ij}. In this section we will make this concrete by specifying this metric accompanied with the coordinate transformation. This will give use real formulas to work with in our simulations in Mathematica. The coordinate transformation which achieves the geometry in Figure 2.1 is best described in curvilinear coordinates as: $r \to r^\star = g(r) = R_1 + r(R_2 - R_1)/R_2$ or $r = R_2(r^\star - R_1)/(R_2 - R_1)$. Here we see that we have a problem with the origin $(\vec{0})$, we will ignore this for now. At a later moment we will come back to this. The metric in curvilinear coordinates is given by:

$$ds^2 = dx^2 + dy^2 + dz^2 = dr^2 + r^2 d\theta^2 + dz^2. \tag{3.21}$$

Hence the metric tensor in curvilinear coordinates is given by: $g_{ij} = diag(1, r^2, 1)$. Making the coordinate transformation:

$$\rho = \begin{pmatrix} r \\ \theta \\ z \end{pmatrix} \to \rho^\star = \begin{pmatrix} g(r) \\ \theta \\ z \end{pmatrix}, \tag{3.22}$$

the metric transforms as:

$$g^\star_{\alpha\beta} = \frac{\partial \rho^i}{\partial \rho^{\star\alpha}} \frac{\partial \rho^j}{\partial \rho^{\star\beta}} g_{ij}(\rho^\star). \tag{3.23}$$

Under our transformation this new metric becomes: $g^\star_{\alpha\beta} = diag(1, r^{\star 2}, 1) = diag(g^{'}(r)^2, g(r)^2, 1)$. Now, with this metric we write Equations 3.18 as:

$$\begin{aligned}
\Lambda^{rr}(r) &= (g^{rr})^2\Lambda = \Big(\frac{R_2 - R_1}{R_2}\Big)^2 \Lambda; \\
\Lambda^{\theta\theta}(r) &= \frac{(g^{\theta\theta})^2}{r^2}\Lambda = \Big(\frac{r^2(R_2 - R_1)^2}{R_2^2(r - R_1)^2}\Big)\Lambda; \\
B(r) &= 1, \\
\beta^r(r) &= \Lambda\Big(\frac{1}{\sqrt{g}}\partial_r[\sqrt{g}g^{rr}] - \frac{1}{r}\Big) + \beta_r g^{rr} = -\frac{1}{r} + \frac{(R_2 - R1)^2}{(r - R_1)R_2^2},
\end{aligned} \tag{3.24}$$

where we set $\Lambda, B = 1$ and $\beta_r = 0$. In Cartesian coordinates these formulas become:

$$\begin{aligned}
\Lambda^{xx}(x,y) &= \frac{(R_2 - R_1)^2}{R_2^2}\Big(\frac{x^2}{x^2 + y^2} + \frac{y^2}{(R_1 - \sqrt{x^2 + y^2})^2}\Big); \\
\Lambda^{xy}(x,y) &= \Lambda^{yx}(x,y) = \frac{(R_2 - R_1)^2 xy}{R_2^2}\Big(\frac{1}{x^2 + y^2} - \frac{1}{(R_1 - \sqrt{x^2 + y^2})^2}\Big); \\
\Lambda^{yy}(x,y) &= \frac{(R_2 - R_1)^2}{R_2^2}\Big(\frac{y^2}{x^2 + y^2} + \frac{x^2}{(R_1 - \sqrt{x^2 + y^2})^2}\Big), \\
B(x,y) &= 1; \\
\beta^x(x,y) &= \frac{x}{\sqrt{x^2 + y^2}}\Big(\frac{(R_2 - R_1)^2}{R_2^2(\sqrt{x^2 + y^2} - R_1)} - \frac{1}{\sqrt{x^2 + y^2}}\Big), \\
\beta^y(x,y) &= \frac{y}{\sqrt{x^2 + y^2}}\Big(\frac{(R_2 - R_1)^2}{R_2^2(\sqrt{x^2 + y^2} - R_1)} - \frac{1}{\sqrt{x^2 + y^2}}\Big).
\end{aligned} \tag{3.25}$$

To give a notion how Equations 3.25 behave spatially, we plot them in Figure 3.1. Here, is seen that around the radius R_1 the changes in the exchange interaction Λ are the largest, as we approach R_2 the exchange interaction becomes more uniform.

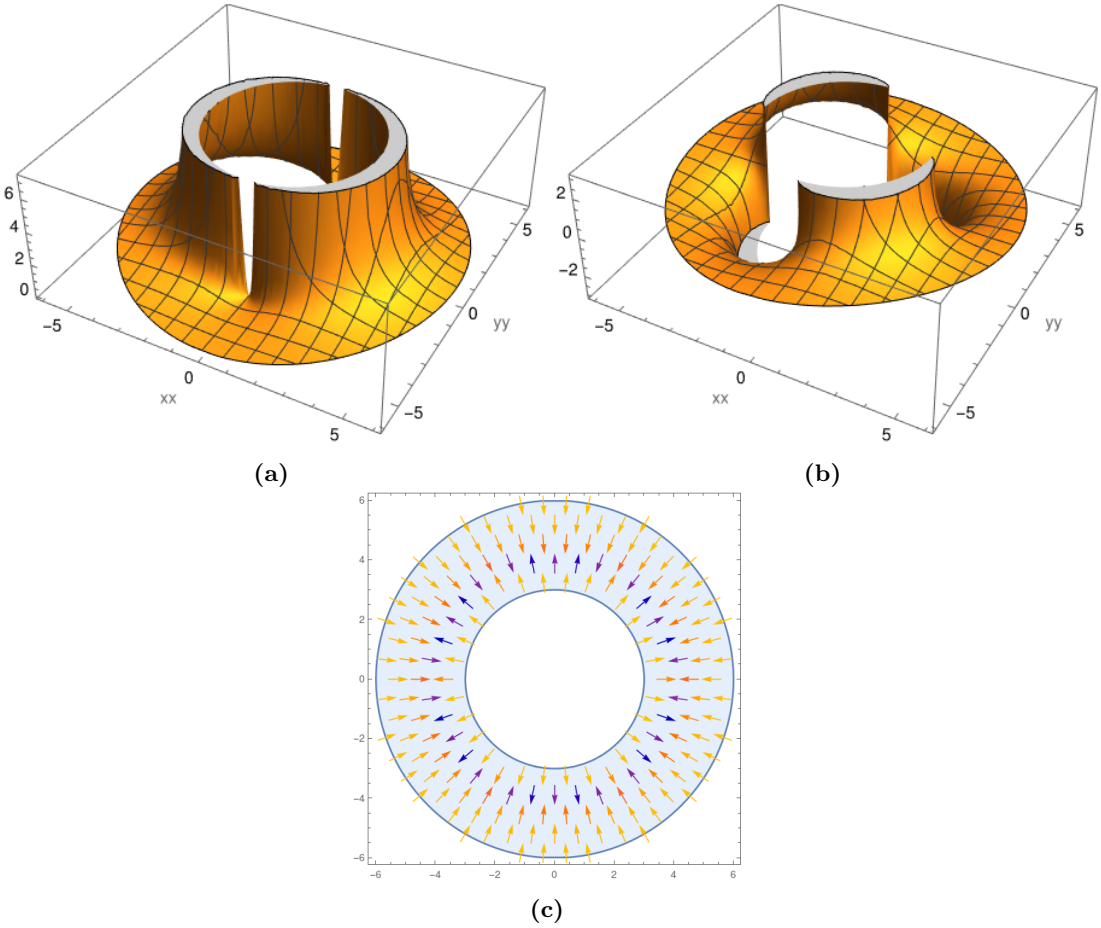

Figure 3.1: Equations 3.25 plotted. (a) $\Lambda^{yy}(x,y)$, (b) $\Lambda^{xy}(x,y) = \Lambda^{yx}(x,y)$ and (c) $(\beta^x(x,y), \beta^y(x,y))$.

3.3.3 Group velocity

We can get some intuition for the theory via the group velocity. The group velocity is the velocity of the incoming waves. It is defined by:

$$v_k = \frac{\partial \omega_k}{\partial k}. \tag{3.26}$$

With this definition and Equation 3.11 we write the group velocity as:

$$(v_k)^i = \Lambda^{ij} k_j - \beta^i. \tag{3.27}$$

In Figure 3.2 we have plotted this vector field. Here, an incoming wave ($\vec{k} = (1,0)$) is used. One can clearly see that this wave is bend around the hole, thus cloaking the area in between.

Also one of the flaws is immediately seen. Since the transformation $\mathbb{R}^2 \to \mathbb{R}^2 \setminus \{0\}$ is not a homeomorphism, an incoming wave at $k^y = 0$ cannot be bend around the hole, thus making a perfect cloak impossible. We will see in simulations that this is negligible.

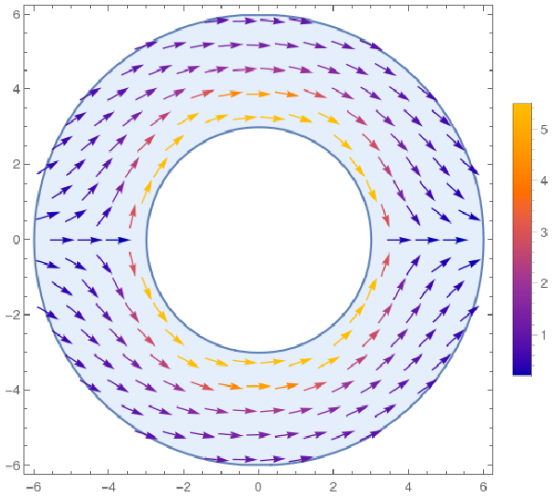

Figure 3.2: The group velocity of an incoming wave with wavenumber $\vec{k} = (1, 0)$ in the cloaking medium. The bar on the right denotes the speed of the wave amplitudes. Here it is clearly seen that the waves are bend around the hole, thus cloaking a possible object.

3.3.4 Results

To simulate spin waves, we have used Mathemtica. Here, we used the function NDSolveValue to solve Equation 3.20. An incoming wave was generated via the function $Exp[-(x-x_{min})^2 - i\omega t]$. In the middle a magnetic core was placed with radius $R_1 = 3$, this core has magnetization $m = 0$ (thus is fully magnetized along the $\hat{z}$ axis). To achieve this we used Dirichlet boundary conditions around the boundary of the hole and Neumann boundary conditions every else. A graphical depiction of the boundary conditions is seen in Figure 3.3. Here, Neumann boundary conditions state that spins will follow the same alignment as the spins at the boundary. Dirichlet boundary conditions state that the spins point in the one direction, no matter how the spin is pointing at the boundary.

Figure 3.3: (a) Neumann boundary conditions for spins. (b) Dirichlet boundary conditions for spins. Spins on the left are real spins in the system, while spins on the right are the stipulated boundary conditions. The spins for the Neumann boundary conditions will follow the same direction the spin is pointing at the boundary. Spins for the Dirichlet boundary condition will always point in one direction, no matter how the spin at the boundary is pointing.

A cloaking region was used of $R_2 = 6$. In this region the material had anisotropic exchange interactions. We limited the strength of the exchange interaction by $|\Lambda| < 2$, which improved the results slightly and is experimentally more feasible. For a radius larger than R_2 isotropic parameters where used with no varying strengths. Below the results are shown of our spin wave simulations. The figure on the left has only uniform parameters, hence no cloaking. The figure on the right uses the isotropies given by Equations 3.25.

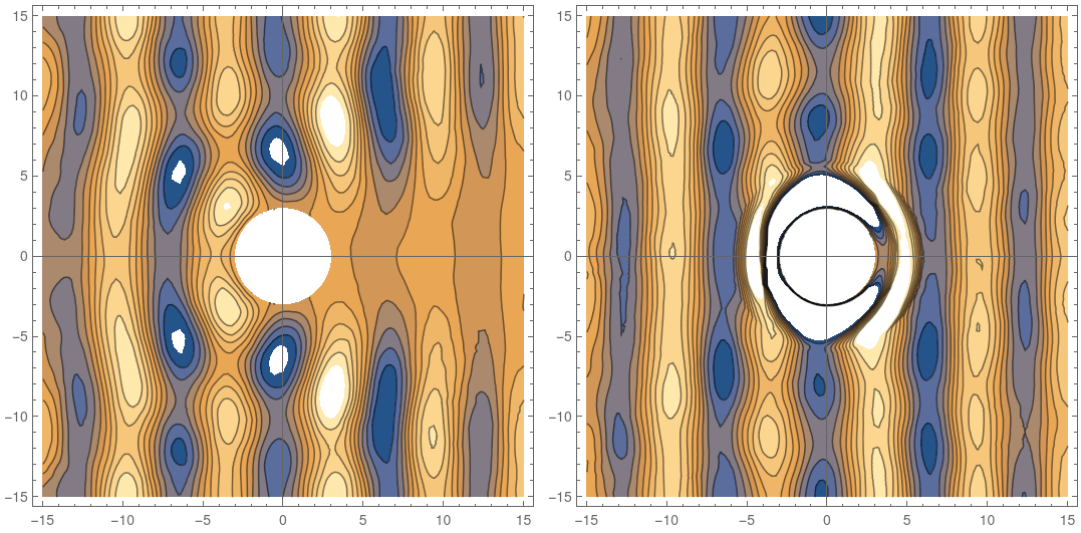

Figure 3.4: (a) Normalized spin waves with no cloaking versus (b) spin waves with a cloaking mechanism. Both propagating from left to right. When there is no cloaking the spin waves interact with the magnetic core. When there is a cloaking mechanism in place, the waves do not interact with the magnetic core. This is seen by comparing the outgoing waves with the incoming ones, in the figure with the cloaking mechanism they are the same.

The differences are clearly seen. When we have no cloaking, the spin waves interact with the magnetic core. This interaction is visualized by the ripple effects as seen on the left of Figure 3.4a and on the right by an absence of spin waves, meaning they were blocked by the core. In Figure 3.4b a cloaking mechanism is used. Here, we see that the spin waves do not interact with the magnetic core. This is seen by comparing the outgoing waves with the incoming ones. In the figure they are the same, thus the cloaking of the magnetic core is achieved. While the spin waves in the cloaking region ($R_1 = 3 < r < R_2 = 6$) have extreme values (white areas denote that the normalized spin waves have amplitudes of 1 or -1), once they leave this area their amplitudes return to normal values.

Chapter 4

Outlook: spin wave cloaking in antiferromagnets

In this chapter we will give an outlook on spin waves in antiferromagnets. Opposed to ferromagnets, antiferromagnets have a zero magnetic moment in their ground state and are thus somewhat the opposite of ferromagnets. This is because their exchange interaction is strictly negative, thus minimizing the Hamiltonian given by Equation 3.1 by ordering their spins antiparallel. A graphical depiction of this can be seen in Figure 4.1a. Here is seen that the spins are alternating in their alignment. To describe spin waves in an antiferromagnet we will consider the unit cell of an up and down spin together, both on their respective lattices m_1 and m_2.

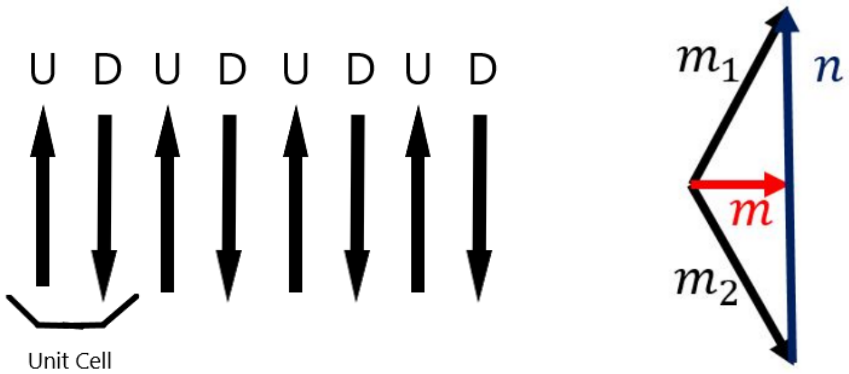

(a) **(b)**

Figure 4.1: (a) Graphical depiction of an antiferromagnet. (b) Graphical depiction of the magnetization and Néel vector (Taken from Kromin, 2021).

Often these unit cells are described in terms of the magnetization and the Néel vector ($\vec{m}$ and $\vec{n}$, respectively). A graphical depiction of the two is seen in Figure 4.1b. Formula wise they are given by: $\vec{m} = (m_1 + m_2)/2$ and $\vec{n} = (m_1 - m_2)/2$. To describe spin waves in an antiferromagnet we will exclusively follow Kromin, 2021. In this paper they consider the antiferromagnet as a combination of two ferromagnetic sublattices (U and D), as seen in Figure 4.1a. The equations of motion of spin waves in these ferromagnetic sublattices are given as before by:

$$\dot{\vec{m}}_{1/2} = \gamma \vec{m}_{1/2} \times \vec{H}_{eff} - \vec{\nu}\partial\vec{m}_{1/2} + \beta\vec{m}_{1/2} \times \vec{\nu}\partial\vec{m}_{1/2}, \tag{4.1}$$

where a spin transfer torque was considered again, with $\vec{\nu}$ the spin current and β the damping parameter. These equations of motions are then described in both Néel and magnetization vectors, using that $\vec{m}_1 = \vec{m} + \vec{n}$ and $\vec{m}_2 = \vec{m} - \vec{n}$:

$$\begin{aligned} \dot{m} &= \gamma m \times \frac{\delta E}{\delta m} + \gamma n \times \frac{\delta E}{\delta n} - \vec{\nu}\partial m + \beta(m \times \vec{\nu}\partial m + n \times \partial n), \\ \dot{n} &= \gamma m \times \frac{\delta E}{\delta n} + \gamma n \times \frac{\delta E}{\delta m} - \vec{\nu}\partial n + \beta(n \times \vec{\nu}\partial m + m \times \partial n). \end{aligned} \tag{4.2}$$

Equations 4.2 now describe the time evolution of two ferromagnetic sublattices, coupled by an interlattice exchange interaction. To make Equations 4.2 more concrete, a free energy contribution is used as:

$$E = \int dV (2A(\partial\vec{n})^2 + 2\lambda(1 - n_x^2) + \epsilon\vec{m}^2). \tag{4.3}$$

Here, the first term is the exchange energy, the second term is an isotropic term and the last term is a magnetic field term. From this free energy, via the variational principle, the effective field terms are expressed as:

$$\frac{\delta E}{\delta m} = 2\epsilon m; \qquad \frac{\delta E}{\delta n} = -4An \times (\partial^2 n \times n) - 4\lambda n_x n \times (\hat{x} \times n). \tag{4.4}$$

These effective field terms are used in Equations 4.2. A ground state of $\vec{n} = \pm\hat{x}$ is considered, we can expand around this ground state. Both, the magnetization and Néel vector can then be expressed as $\vec{n} = \hat{x} + (0, \delta n_y, \delta n_z)^T = \hat{x} + \vec{h}$ and $\vec{m} = \delta(m_x, m_y, m_z)^T$. Using these expansions, the equations of motion are expressed as:

$$\begin{aligned} \dot{\vec{m}} &= -4A\gamma\nabla^2\vec{h} + 4\lambda\gamma\vec{h} + \vec{\nu} \cdot \nabla(\beta\vec{h} - \vec{m}) \\ &\to -4A\gamma\nabla^2\vec{h} + 4\lambda\gamma\vec{h} + \vec{\xi} \cdot \nabla\vec{h}, \\ \dot{\vec{h}} &= -\vec{\nu} \cdot \nabla(\beta\vec{m} - \vec{h}) - 2\epsilon\gamma\vec{m} \\ &\to -\vec{\xi} \cdot \nabla\vec{m} - 2\epsilon\gamma\vec{m}, \end{aligned} \tag{4.5}$$

where we decoupled the adiabatic and non-adiabatic spin transfer torque in both the second equations, like we did in the ferromagnetic case. This is the final result of Kromin, 2021. Now, we will express this result in curved coordinates. To do this, we will first calculate the second time derivative of the magnetization $\vec{m}$ and eliminate the vector $\vec{h}$ in this expression. This results in the following equation of motion:

$$\begin{aligned} \ddot{\vec{m}} &= -4A\gamma\nabla^2\dot{\vec{h}} + 4\lambda\gamma\dot{\vec{h}} + \vec{\xi} \cdot \nabla\dot{\vec{h}} \\ &= 8A\gamma^2\epsilon\nabla^2\vec{m} - 8\epsilon\gamma^2\lambda\vec{m} - 2\epsilon\gamma\vec{\xi} \cdot \nabla\vec{m} - \xi^2\nabla^2\vec{m}. \end{aligned} \tag{4.6}$$

We can group these parameters in dimensionless terms, to make discussing them more easy:

$$\ddot{\vec{m}} = A\nabla^2\vec{m} - B\vec{m} - \vec{\beta}\nabla\vec{m}. \tag{4.7}$$

The equation we can write in flat coordinates as:

$$\partial_t^2 m^i = A\partial_j^2 m^i - Bm^i - \beta^j \partial_j m^i \tag{4.8}$$

and in curved coordinates as:

$$\partial_t^2 \Lambda_i^u m^i = A\bigstar m^i - B\Lambda_i^u m^i - \beta_\nu g^{\nu j}\partial_j(\Lambda_i^u m^i). \tag{4.9}$$

From Moon and Spencer, 1953 and using a diagonal metric, the vector Laplacian $\bigstar m^i$ is equal to:

$$\begin{aligned}\bigstar m^1 = \hat{e}_1\Big\{ &\frac{1}{\sqrt{g_{11}}}\partial_1\Big[\frac{1}{\sqrt{g}}\partial_1\Big(\sqrt{g}g^{11}m_1\Big)\Big] + \frac{1}{\sqrt{g_{11}}}\partial_1\Big[\frac{1}{\sqrt{g}}\partial_2\Big(\sqrt{g}g^{22}m_2\Big)\Big] \\ &+ \frac{1}{\sqrt{g_{11}}}\partial_1\Big[\frac{1}{\sqrt{g}}\partial_3\Big(\sqrt{g}g^{33}m_3\Big)\Big] - \sqrt{\frac{g_{11}}{g}}\partial_2\Big[\frac{g_{33}}{\sqrt{g}}\partial_1\Big(\sqrt{g_{22}m_2}\Big)\Big] \\ &+ \sqrt{\frac{g_{11}}{g}}\partial_2\Big[\frac{g_{33}}{\sqrt{g}}\partial_2\Big(\sqrt{g_{11}m_1}\Big)\Big] + \sqrt{\frac{g_{11}}{g}}\partial_3\Big[\frac{g_{22}}{\sqrt{g}}\partial_3\Big(\sqrt{g_{11}m_1}\Big)\Big] \\ &- \sqrt{\frac{g_{11}}{g}}\partial_3\Big[\frac{g_{22}}{\sqrt{g}}\partial_1\Big(\sqrt{g_{33}m_3}\Big)\Big]\Big\},\end{aligned} \tag{4.10}$$

where we only showed the vector Laplacian $\bigstar$ for the first coordinate. This vector Laplacian causes a big problem, because it is a lot more complex than the scalar case (Equation 2.12). Even if Equation 4.9 can be simplified with demanding that $\partial_j \Lambda_i^\mu = 0$, which is the case for our cloaking transformation, dealing with this vector Laplacian is very difficult. To build a cloaking mechanism or even a simple wave guide, one has to try to find a geometry that greatly simplifies Equation 4.10. Even if one finds such a geometry, there is a great change that the anisotropies one finds are more difficult than in the ferromagnetic case.

Chapter 5

Discussion and conclusion

5.1 Conclusion

In the first part of this thesis we tried to give a notion of transformation optics and how it can be used to manipulate wave propagation. We explained that there is a connection between curvature and anisotropic material parameters and the influence they have on wave propagation. This connection was found as a relation between transformation optics and general relativity, where general relativity describes wave propagation in curved space and transformation optics in an anisotropic medium. The notion of geodesics and the metric they come with was of utmost importance to try to find anisotropies to influence wave propagation. With this newfound theory of transformation optics we discussed electromagnetic wave propagation and ways to cloak objects from these electromagnetic waves. We strengthened these ideas by showing simulations and experimental results. Both showing that cloaking could be achieved for electromagnetic waves.

Then we considered spin wave propagation in ferromagnets. Here, we considered the continuous vector field of the magnetization and derived the equations of motion for the spin waves. We linearized these equations to compare them to the electromagnetic example, where we found a problem. This problem, we solved by introducing a spin transfer torque. From our cloaking geometry we got numerical results for the anisotropic exchange interaction and the spin transfer torque, with wich we could illustrate our theory via the group velocity. Lastly, we simulated the results in Mathematica, which showed that theoretically a cloaking mechanism can be build for spin waves in ferromagnets.

As an outlook, we looked at spin waves in anitferromagnets. From Kromin, 2021 we got the equations of motion, which we wrote as one equation with a double time derivative in the magnetization. This equation we again tried to write in curved coordinates, but the vector Laplacian posed a problem. Instead of the scalar Laplacian in curved coordinates, which is expressed as a relative simple function, the vector Laplacian is expressed much more complex. Hence, in further research a geometry has to be found such that this vector Laplacian is vastly reduced in complexity, to arrive at feasible results for anisotropic parameters.

5.2 Discussion and outlook

This thesis was inspired by the paper of Elyasi et al., 2016, here they build a cloaking device by introducing anisotropies in the gyromagnetic ratio (γ) or saturation magnetization (M_s). In the paper their cloaking condition was based on the magnetization vector, where the equations of motion should remain invariant under the transformation $\vec{M}_d(\vec{\rho}) \rightarrow T\vec{M}_d'(\vec{\rho}')$. The $'$ denotes curved coordinates. We on the other hand linearized the equations of motion first and then derived our anisotropies. Their results were therefore different to ours. While their results were maybe more feasible, we achieved better cloaking overall. Further research has to prove which implementation of cloaking devices delivers better results in experimental settings.

Overall we used simplified equations of motion for the propagation of spin waves. One of the things that was omitted was Gilbert damping, this damping was set to zero. To formulate a more complete theory one could include Gilbert damping. For further research it has to be investigated what effect including this damping has on the anisotropies found and if it is really of importance, since spin waves are much more robust than electromagnetic waves. It is found that electromagnetic wave distortion is in the scale of pico seconds, while for spin waves it is in the scale of nano or mirco seconds Mahmoud et al., 2020.

Even with a simplified version of the equations of motion, we found a lot of anisotropies and there is a possibility that not all parameters found are physical. For instance, we had to introduce a negative exchange in some areas. Experimentally these negative exchange interactions are found Kumar and Yusuf, 2015, but it has to be investigated further if they also could occur in anisotropic exchange interactions. This discussion raises the question of the overall feasibility of the anisotropic parameters we have found. While, experimentally anisotropic exchange interactions are found Kavokin, 2001; Gor'kov and Krotkov, 2003; Kavokin, 2004; Li and You, 2014, successive research has to address their feasibility in building cloaking devices. If non-physical anisotropic parameters are found, other anisotropic parameters have to be chosen. This is possible since in this research the anisotropic exchange is chosen arbitrarily and other parameters can be chosen. These can include the saturation magnetization (M_s) or the gyromagnetic ratio (γ). It is maybe even possible to make combinations of the three. Another way to solve the feasibility of anisotropic parameters is to look at other cloaking geometries, which possible can reduce the need of anisotropies and thus facilitate the feasibility of experiments.

The propagation of spin waves was simulated in Mathematica. This is the simplest way to simulate them, since Mathematica solves the equations of motion we used to derive these anisotropies. It is far more preferable to derive the anisotropies from the equations of motion and then simulate spin wave propagation in a real spin system. This, for instance, can be done in a program like Mumax3 which is specialized for spin wave simulations. Mumax3 can deal with all kind of interactions which Mathematica is not build for Vansteenkiste et al., 2014. Sadly, it is not yet possible to simulate anisotropic exchange in Mumax3, rendering this option impossible at the moment.

Lastly, it is maybe of importance to state that cloaking devices are an extreme example of the use of transformation optics and have few uses in building spintronic devices. Theoretically they can perfectly illustrate the use of transformation optics and the validation of these cloaking devices, but are experimentally not a goal to be pursued. A much more feasible use of transformation optics is in the creation of wave guides. These guides can be used to facilitate building logic gates for spin waves and uses less extreme geometries needing less anisotropic parameters.

Acknowledgements

I would like to thank Rembert and Joren for their guidance throughout this project. The discussions we had were always very helpful. Both discussions about physics as well as the discussions about racing bikes, since they brought a relaxed atmosphere and a fascinating insight in a subject I knew nothing about.

Bibliography

[1] Andrii V Chumak et al. "Magnon spintronics". In: *Nature physics* 11.6 (2015), pp. 453–461. DOI: https://doi.org/10.1038/nphys3347.

[2] Steven A. Cummer et al. "Full-wave simulations of electromagnetic cloaking structures". In: *Phys. Rev. E* 74 (3 Sept. 2006), p. 036621. DOI: 10.1103/PhysRevE.74.036621. URL: https://link.aps.org/doi/10.1103/PhysRevE.74.036621.

[3] Mehrdad Elyasi et al. "Cloaking the magnons". In: *Phys. Rev. B* 93 (10 Mar. 2016), p. 104418. DOI: 10.1103/PhysRevB.93.104418. URL: https://link.aps.org/doi/10.1103/PhysRevB.93.104418.

[4] L. P. Gor'kov and P. L. Krotkov. "Spin relaxation and antisymmetric exchange in n-doped III-V semiconductors". In: *Phys. Rev. B* 67 (3 Jan. 2003), p. 033203. DOI: 10.1103/PhysRevB.67.033203. URL: https://link.aps.org/doi/10.1103/PhysRevB.67.033203.

[5] D.T.E. van de Heisteeg. "Quantum fluctuations and phase transitions in antiferromagnetic spin configurations". MA thesis. Utrecht: Utrecht University, July 2016.

[6] K. V. Kavokin. "Anisotropic exchange interaction of localized conduction-band electrons in semiconductors". In: *Phys. Rev. B* 64 (7 July 2001), p. 075305. DOI: 10.1103/PhysRevB.64.075305. URL: https://link.aps.org/doi/10.1103/PhysRevB.64.075305.

[7] K. V. Kavokin. "Symmetry of anisotropic exchange interactions in semiconductor nanostructures". In: *Phys. Rev. B* 69 (7 Feb. 2004), p. 075302. DOI: 10.1103/PhysRevB.69.075302. URL: https://link.aps.org/doi/10.1103/PhysRevB.69.075302.

[8] Raphael Kromin. "Domain wall injection in antiferromagnets". MA thesis. Mainz: Johannes Gutenberg-Universität, July 2021.

[9] Benjamin Krueger. "Current-Driven Magnetization Dynamics : Analytical Modeling and Numerical Simulation". In: 2012.

[10] Amit Kumar and S.M. Yusuf. "The phenomenon of negative magnetization and its implications". In: *Physics Reports* 556 (2015). The phenomenon of negative magnetization and its implications, pp. 1–34. ISSN: 0370-1573. DOI: https://doi.org/10.1016/j.physrep.2014.10.003. URL: https://www.sciencedirect.com/science/article/pii/S0370157314003937.

[11] Ulf Leonhardt and Thomas G Philbin. "General relativity in electrical engineering". In: *New Journal of Physics* 8.10 (Oct. 2006), p. 247. DOI: 10.1088/1367-2630/8/10/247. URL: https://dx.doi.org/10.1088/1367-2630/8/10/247.

[12] Ulf Leonhardt and Thomas G. Philbin. *Transformation Optics and the Geometry of Light*. 2008. arXiv: 0805.4778 [physics.optics].

[13] Rui Li and J. Q. You. "Anisotropic exchange coupling in a nanowire double quantum dot with strong spin-orbit coupling". In: *Phys. Rev. B* 90 (3 July 2014), p. 035303. DOI: 10.1103/PhysRevB.90.035303. URL: https://link.aps.org/doi/10.1103/PhysRevB.90.035303.

[14] Abdulqader Mahmoud et al. "Introduction to spin wave computing". In: *Journal of Applied Physics* 128.16 (Oct. 2020), p. 161101. ISSN: 0021-8979. DOI: 10.1063/5.0019328. eprint: https://pubs.aip.org/aip/jap/article-pdf/doi/10.1063/5.0019328/13990433/161101_1_online.pdf. URL: https://doi.org/10.1063/5.0019328.

[15] Marco Miniaci et al. "Large scale mechanical metamaterials as seismic shields". In: *New Journal of Physics* 18.8 (Aug. 2016), p. 083041. DOI: 10.1088/1367-2630/18/8/083041. URL: https://dx.doi.org/10.1088/1367-2630/18/8/083041.

[16] Parry Moon and Domina Eberle Spencer. "The meaning of the vector Laplacian". In: *Journal of the Franklin Institute* 256.6 (1953), pp. 551–558. ISSN: 0016-0032. DOI: https://doi.org/10.1016/0016-0032(53)91160-0. URL: https://www.sciencedirect.com/science/article/pii/0016003253911600.

[17] *Parallel Transport and Geodesic*. URL: http://www.physicsimplified.com/2013/08/10-parallel-transport-and-geodesic.html.

[18] D. Schurig et al. "Metamaterial Electromagnetic Cloak at Microwave Frequencies". In: *Science* 314.5801 (2006), pp. 977–980. DOI: 10.1126/science.1133628. eprint: https://www.science.org/doi/pdf/10.1126/science.1133628. URL: https://www.science.org/doi/abs/10.1126/science.1133628.

[19] Denis D. Sheka. "A perspective on curvilinear magnetism". In: *Applied Physics Letters* 118.23 (June 2021), p. 230502. ISSN: 0003-6951. DOI: 10.1063/5.0048891. eprint: https://pubs.aip.org/aip/apl/article-pdf/doi/10.1063/5.0048891/16734093/230502_1_online.pdf. URL: https://doi.org/10.1063/5.0048891.

[20] Arne Vansteenkiste et al. "The design and verification of MuMax3". In: *AIP Advances* 4.10 (Oct. 2014), p. 107133. ISSN: 2158-3226. DOI: 10.1063/1.4899186. eprint: https://pubs.aip.org/aip/adv/article-pdf/doi/10.1063/1.4899186/12878560/107133_1_online.pdf. URL: https://doi.org/10.1063/1.4899186.